J. Synchrotron Rad. (1997). **4**, 185–190

X-ray Reflectivity Study of Semiconductor Interfaces

M. K. Sanyal,[a] A. Datta,[a] S. Banerjee,[a] A. K. Srivastava,[b] B. M. Arora,[b] S. Kanakaraju[c] and S. Mohan[c]

[a]Saha Institute of Nuclear Physics, 1/AF Bidhan Nagar, Calcutta-700 064, India, [b]Tata Institute of Fundamental Research, Colaba, Mumbai-400 005, India, and [c]Indian Institute of Science, Bangalore-560 012, India. E-mail: milan@hpl.saha.ernet.in

(*Received 6 August 1996; accepted 11 December 1996*)

The results of an X-ray reflectivity study of thick AlAs–AlGaAs and thin Ge–Si–Ge multilayers grown using metal-organic vapour-phase epitaxy and ion-beam sputtering deposition techniques, respectively, are presented. Asymmetry in interfaces is observed in both of these semiconductor multilayers. It is also observed that although the Si-on-Ge interface is sharp, an $Si_{0.4}Ge_{0.6}$ alloy is formed at the Ge-on-Si interface. In the case of the III–V semiconductor, the AlAs-on-AlGaAs interface shows much greater roughness than that observed in the AlGaAs-on-AlAs interface. For thin multilayers it is demonstrated that the compositional profile as a function of depth can be obtained directly from the X-ray reflectivity data.

Keywords: X-ray reflectivity; semiconductor multilayers; interfacial diffusion.

1. Introduction

Semiconductor multilayers consist of a periodic sequence of alternately grown layers of two different semiconductor materials. By tuning the growth parameters of these materials a number of devices have been fabricated, and it is expected that, apart from the development of new devices having novel optical and transport properties (Presting *et al.*, 1992), mastering the growth–characterization–growth cycle will open up the possibility of sharpening our understanding in low-dimensional physics. To achieve this goal of designing multilayers having a prescribed electronic structure (so-called 'band-structure engineering'), one must characterize the interfacial structure of grown multilayers with atomic resolution.

Interfacial structures in semiconductor multilayers grown by sequential processes play a very important role in their physical properties (Pan *et al.*, 1996; Tan, Jagadish, Williams, Zou & Cockayne, 1996; Dandrea, Duke & Zunger, 1992; Foulon, Priester, Allan, Garcia & Landesman, 1992). During such *ABAB*... multilayer growth, the *A*-on-*B* interface may be abrupt whereas the *B*-on-*A* interface may be diffuse (Froyen & Zunger, 1996; Bode & Ourmazd, 1992; Moison, Guille, Houzay, Barthe & Van Rompay, 1989), and, in general, achievement of atomically abrupt interfaces in multilayers is critically dependent on interfacial diffusion and mixing (Chen, Xiao, Au, Zhou & Loy, 1996; Spencer, Menéndez, Pfeiffer & West, 1995; Kohleick, Förster & Lüth, 1993; Stall, Zilko, Swaminathan & Schumaker, 1985). Various techniques are available to characterize the depth profile of the film, such as secondary-ion mass spectrometry, Auger electron spectroscopy and X-ray photoelectron spectroscopy. Most of these techniques are destructive and have various unwanted effects, such as preferential removal rates, intermixing and alloying during the analysis process. X-rays, due to their penetrative power and ability to resolve variations at atomic length scales, provide a wide range of techniques to characterize the structures of multilayers.

Although a detailed X-ray diffraction study is essential to understand the structural details of multilayer interfaces, the X-ray reflectivity technique can be a very convenient probe for rapid completion of the growth–characterization–growth cycle (Sinha *et al.*, 1994). In this technique one obtains the electron-density profile (EDP), averaged over the *xy* plane, as a function of depth, *i.e.* exactly opposite to the growth direction (given by *z*, with $z = 0$ at the surface and increasing positively along the depth). As this is a non-destructive technique and can provide us with information (Sanyal *et al.*, 1993; Schlomka *et al.*, 1996) regarding the interfacial roughnesses, uniformity of the layer thicknesses *etc.*, this technique may soon become a standard tool in multilayer research.

In X-ray reflectivity studies one measures the intensity of a specularly reflected (angle of incidence = angle of scattering) X-ray beam as a function of incident angle and plots it as a function of the wavevector, k [$= q_z/2 = (2\pi/\lambda)\sin\theta$, where θ is the angle of incidence], to obtain a reflectivity profile of a sample. The periods of various oscillations, separation of multilayer peaks and their relative intensities, in the reflectivity profile, provide us with information regarding the various thicknesses associated with the film, bilayer thicknesses and the contrasts in their electron densities, respectively. The separation of multilayer peaks is inversely proportional to the corresponding bilayer thickness and, as a result, most of the work performed so far in multilayers using this technique involves multilayers having small bilayer thicknesses (~100 Å).

On the other hand, multilayer systems for devices, especially for optoelectronic applications, have layer thick-

nesses typically of ~1000 Å, only four to eight times less than optical wavelengths. The device performance strongly depends on the quality of the different layers in multilayers, which in turn depends on the growth process. Characterizing the chemical profile of a multilayer film across the depth with ångström resolution is of immense technological importance.

In this communication we present high-resolution X-ray reflectivity studies of two types of semiconductor multilayers, having *thin* (~100 Å) and *thick* (~1000 Å) bilayers. The thin samples used are Ge–Si–Ge trilayers grown by ion-beam sputtering deposition. An AlAs–AlGaAs multilayer sample having 16 bilayers (~1000 Å each) grown by metal-organic vapour-phase epitaxy was used as the thick sample. The systems presented in this communication cover the applicability of the X-ray reflectivity technique for wide-ranging semiconductor multilayer systems, important for various technological applications.

The conventional method of extracting the EDP from the reflectivity profile is based on an iterative solution of Fresnel equations subsequently modified to account for interfacial roughnesses (Parratt, 1954; Piecuch & Nevot, 1990). This technique gives very good results for systems where the actual EDP is close to the *a priori* assumption of the EDP with which the non-linear fitting procedure is started and only a few parameters are involved in the fit. Owing to the iterative non-linear relationship between the reflectivity profile and real-space parameters, the determination of the latter by fitting is difficult when the initial assumption of the EDP is far from the actual solution.

Analysis of the interfacial profile of a multilayer, especially to investigate mixing and diffusion at interfaces, is much facilitated if a scheme which does not depend on the initial assumption of the EDP is available. We have developed such a method based on the distorted wave Born approximation (Sanyal, Basu, Datta & Banerjee, 1996), which can detect small variations in the EDP from the measured reflectivity profile. This method has been used here to study the Ge–Si–Ge trilayer. In this scheme, first the exact reflectance of a system, consisting of substrate and a uniform thin film of the same thickness and average electron density as the film under investigation, is calculated. This information is used to determine the variation of electron density as a function of depth in this film by using a perturbative scheme (see §4 and Sanyal *et al.*, 1993). However, in systems like this thick multilayer, the presence of the substrate is not felt due to the high X-ray absorption coefficients of these materials. As a result, this method cannot work and hence the conventional technique has been used for the analysis of the thick AlAs–AlGaAs multilayers (see §3). It should be mentioned here that the reflectivity profile calculated using the conventional technique basically represents the top few bilayers of this multilayer sample. The availability of intense high-energy photon sources at third-generation synchrotrons will provide us with data sensitive to larger numbers of bilayers in this type of thick multilayer.

2. Experimental details

The $Al_{0.5}Ga_{0.5}As$–AlAs multilayer sample used in this work was grown by low-pressure metal-organic vapour-phase epitaxy at 100 Torr and 973 K using trimethyl gallium, trimethyl aluminium and arsine as the source materials. The substrate used for growth was (100)-oriented n^+ GaAs. The typical growth rate for AlAs was kept at ~5 Å s^{-1} and for AlGaAs at ~10 Å s^{-1}. The structure was grown for a 16-period $\lambda/4$ Bragg reflector with nominal thicknesses of the AlAs layer of ~500 Å and the AlGaAs layer of ~440 Å, in each period, adjusted according to the refractive index values of the two materials at the wavelength of interest (6330 Å).

Before depositing Si–Ge samples, the Si (001) single-crystal substrates were cleaned by vapour degreasing and then dipped in 10% HF to remove the native oxide and subsequently rinsed in flowing de-ionized water. The substrates were then loaded in the vacuum chamber with a target-to-substrate distance of 8 cm. The ion beam sputtering deposition system employs a Kauffman-type ion source of 3 cm diameter. The Ar-ion beam with an energy of 1 keV and current of 3 mA intensity is incident on the target at an angle of 50° to the target surface normal. During the sputtering the pressure in the chamber was maintained at 3×10^{-5} Torr. Films were deposited onto the substrates maintained at 373 K (sample 1) and 673 K (sample 2), with deposition rates of 0.3 and 0.26 Å s^{-1} for Si and Ge, respectively. The nominal thickness of the layer was estimated to be ~35 ± 3 Å for Si and 35 ± 4 Å for Ge.

X-ray reflectivity measurements were performed using a high-resolution diffractometer (Optix Microcontrole) with Cu $K\alpha_1$ X-rays obtained from a 18 kW rotating-anode (Enraf Nonius FR591) X-ray generator and Si (111) monochromator.

3. Thick multilayer: AlAs–AlGaAs

We collected high-resolution X-ray reflectivity data of this system with a q_z step-size of 0.00014 $Å^{-1}$ (0.001° with Cu $K\alpha_1$ radiation) and with a q_z resolution of 0.0018 $Å^{-1}$. The collected data were analyzed using a conventional scheme based on Parratt formalism (Parratt, 1954). Our sample is a 16-bilayer stack sitting on a GaAs substrate. The top layer of the stack is AlGaAs and the bottom layer is AlAs. We have assumed that all the AlGaAs layers are identical, and that the AlAs layers are identical. For such a multilayer film, the EDP along the depth is given by (Piecuch & Nevot, 1990)

$$\rho(z) = \rho_G f(z_1, \sigma_0) + (\rho_A - \rho_G) \sum_{i=1}^{7} f(z_{2i}, \sigma_G) + (\rho_G - \rho_A) \sum_{i=1}^{7} f(z_{2i+1}, \sigma_A) + (\rho_s - \rho_A) f(z_{16}, \sigma_s), \quad (1)$$

where the subscripts 0, s, A and G refer to air, substrate, AlAs layer and AlGaAs layer, respectively, ρ_u is the average electron density of medium u, and σ_u is the 'roughness' of the interface of medium u on medium v expressed as the 'error function'

$$f(z_l, \sigma) = f(z - z_l, \sigma) = \sigma^{-1}(2\pi)^{-1/2} \int_{-\infty}^{z - z_l} \exp(-t^2/2\sigma^2)\, dt, \quad (2)$$

where z_l is the position of the lth interface in the multilayer.

The data analysis was performed by fitting to a reflectivity profile calculated with this modified Parratt scheme (Parratt, 1954) where the error functions are Debye–Waller-like functions (Rao & Sanyal, 1994). Electron densities, layer thicknesses and three r.m.s. roughnesses, namely air-on-AlGaAs (σ_0), AlGaAs-on-AlAs (σ_G) and AlAs-on-AlGaAs (σ_A), were used as fitting parameters. Owing to a lack of penetration of X-rays in grazing-incidence geometry, the calculated profile was not sensitive to the AlAs-on-substrate roughness. In fact, the profile was not sensitive to changes after the first four bilayers. All the above-mentioned parameters were assumed to be identical for all bilayers of the sample except for the top layer. However, as can be seen from Fig. 1(*a*), the calculated reflectivity has higher values than those observed in the q_z range 0.05–0.2 Å^{-1}. Owing to high sensitivity and expected modification due to exposure to ambient conditions, the top AlGaAs layer was modelled using 20 Å boxes. The resultant fit is thereby much improved (see Fig. 1*b*).

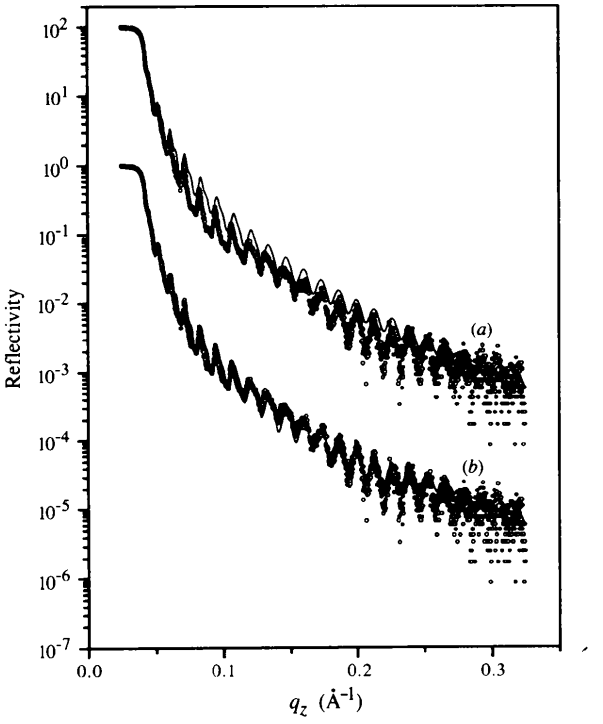

Figure 1
X-ray reflectivity data (shown in dots) of the $Al_{0.5}Ga_{0.5}As$–AlAs multilayer. The fit (shown in solid lines) was obtained (*a*) without and (*b*) with modification of the top 80 Å (see text for details).

The fitted profile gives the correct value of q_c, decided primarily by the thick top AlGaAs layer. The calculated profile gives the correct periodicities of the multilayer peaks in the reflectivity profile and matches the observed shapes of the oscillation peaks quite closely. The thicknesses of the $Al_{0.5}Ga_{0.5}As$ and AlAs layers are found to be 465.9 and 471.7 Å, respectively, and their electron densities 1.17 and 0.93 e Å^{-3}, respectively. These electron densities are almost the same as those of the corresponding perfect crystals having the same composition.

The obtained EDP of the multilayer is shown in Fig. 2. At the top surface (inset *A*) we notice that the electron density (expressed in e Å^{-3}) increases from a low value, crosses the average electron density of $Al_{0.5}Ga_{0.5}As$ (1.17 e Å^{-3}) and then returns to this value again. The electron densities of the top four slices of 20 Å each are found to be 1.0, 1.15, 1.20 and 1.20 e Å^{-3}, respectively. The interfacial roughnesses obtained from the fit point to a strong asymmetry: the AlAs-on-AlGaAs interface shows a large r.m.s roughness (σ_A) of 16.9 Å (Fig. 2, inset *C*) whereas the AlGaAs-on-AlAs interface is much sharper with a roughness (σ_G) of 3.5 Å (inset *B*). The air/film interface is found to have a roughness $\sigma_0 \simeq 2.8$ Å. We performed secondary-ion mass-spectrometry measurement of the sample to confirm the asymmetry of the interfacial roughnesses present in the sample and to understand the chemical origin of this asymmetry (Sanyal *et al.*, 1997).

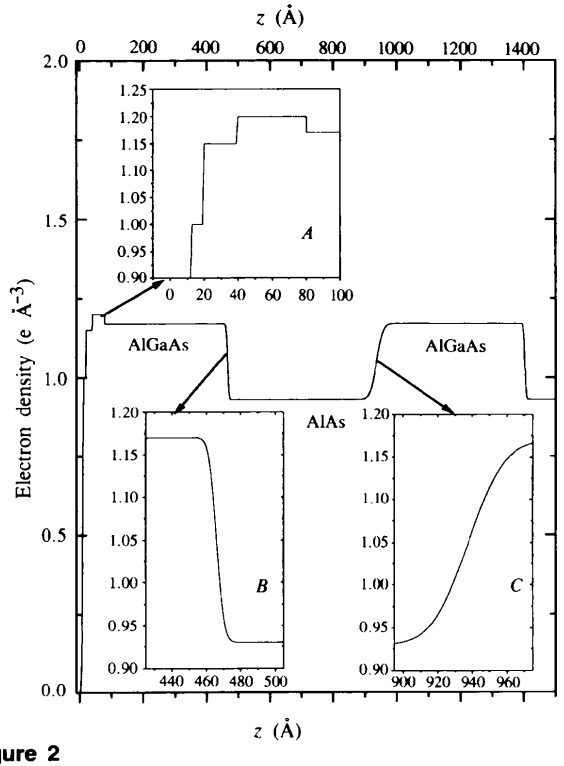

Figure 2
Electron-density profile of the first three layers of the $Al_{0.5}Ga_{0.5}As$–AlAs multilayer. Inset *A* shows the top 100 Å of the $Al_{0.5}Ga_{0.5}As$ layer, inset *B* shows the AlGaAs-on-AlAs interface and inset *C* shows the AlAs-on-AlGaAs interface (see text for details). The electron density is measured in e Å^{-3}.

4. Thin multilayers: Ge–Si–Ge

In Figs. 3(*a*) and 3(*b*) we show the X-ray reflectivity data of Ge–Si–Ge trilayers deposited at 273 K (sample 1) and 673 K (sample 2), respectively. These reflectivity data were analyzed using a scheme, where the film has been considered to be composed of a number of thin slices or boxes of electron density ρ_i. This scheme is based on the distorted wave Born approximation formalism (Sinha, Sirota, Garoff & Stanley, 1988; Sanyal *et al.*, 1993, 1996) and requires one reflectivity profile taken either with laboratory X-ray sources or with a synchrotron source. In this scheme, most of the time, unknown EDPs can be extracted from the specular X-ray reflectivity data without any *a priori* assumption. This scheme has been tested extensively, using simulated data on various model systems, for its sensitivity and ruggedness (Banerjee, Sanyal, Datta, Kanakaraju & Mohan, 1996; Sanyal *et al.*, 1996). The sensitivity of the method to density variations makes the specular X-ray reflectivity technique more powerful. Nevertheless, it should be mentioned here that, unlike the anomalous X-ray reflectivity method (Sanyal *et al.*, 1993; Ohkawa *et al.*, 1996), this scheme involves a fitting process and, as a result, can sometimes produce unphysical EDPs. To avoid these unphysical solutions we calculated all reflectivity profiles using Parratt's (1954) scheme with the EDP obtained from fitting and compared them with the data.

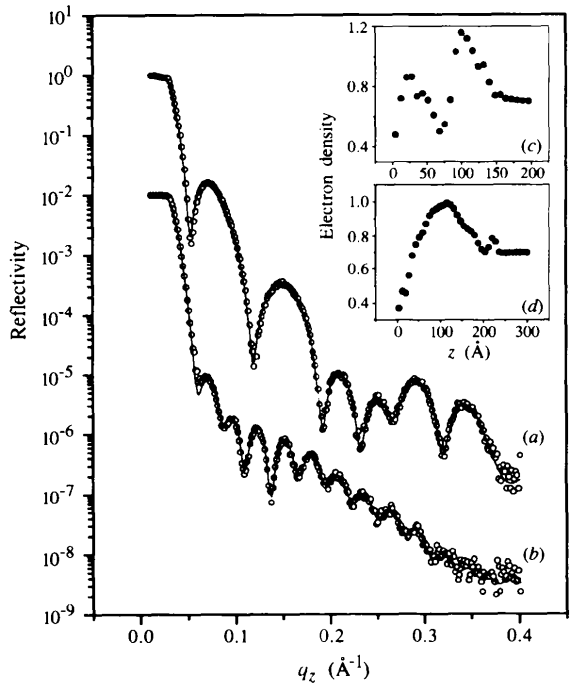

Figure 3
X-ray reflectivity for the Ge–Si–Ge trilayer deposited with substrate temperatures of (*a*) 373 K (sample 1) and (*b*) 673 K (sample 2) [○, data; solid line, fit]. EDPs obtained from the fit to the above data for (*c*) 373 K (sample 1) and (*d*) 673 K (sample 2), respectively.

The calculated reflectivity, as a function of momentum transfer, $R(k)$, can be written in this scheme as

$$R(k) = \left|ir_0(k) + (2\pi b/k)[a^2(k)\Delta\rho(q_z^f) + b^2(k)\Delta\rho^*(q_z^f)]\right|^2, \tag{3}$$

where $r_0(k)$ is the specular reflectance coefficient of the film with average electron density ρ_0, and $\Delta\rho(q_z^f)$ can be written in terms of $\Delta\rho_i$ ($= \rho_i - \rho_0$) of thickness d of the ith box as

$$\Delta\rho(q_z^f) = (i/q_z^f)\left\{\sum_{j=2}^{j=N}(\Delta\rho_j - \Delta\rho_{j-1})\exp[iq_z^f(j-1)d] + \Delta\rho_1 - \Delta\rho_N\exp(iq_z^f Nd)\right\}, \tag{4}$$

where N is the total number of boxes used in the calculation. By selecting an appropriate number of slices and ρ_0 of the film, we fit equation (3) with $\Delta\rho_i$ as the fit parameters after convoluting the data with a Gaussian instrumental resolution function.

The obtained (Banerjee *et al.*, 1996) EDP of sample 1 is shown in Fig. 3(*c*). Since the thickness of the film was overestimated, we detect the substrate starting from 150 Å. The EDP clearly shows three distinct regions: the two electron-density maxima for the Ge layers and a minimum due to the Si layer between the two Ge layers. The obtained electron densities of Ge and Si of the film are found to be low. We also see a lowering of electron density at the surface due to surface roughness. Using this EDP we generated the reflectivity curve using Parratt's (1954) formalism. We show this in Fig. 3(*a*) (solid line) along with the experimental data (open circles). The obtained EDP of sample 2 is shown in Fig. 3(*d*). The substrate starts from 200 Å and we also observe that a strong intermixing has occurred. The first layer of Ge has diffused into the substrate and into the middle Si layer modifying the EDP of the film, as shown in Fig. 3(*c*).

The obtained low electron density of the sample may be due to defects, pinholes, voids, amorphous or poor crystallinity (Lyakas *et al.*, 1995). From the obtained EDP one can estimate the packing fraction of the film as a function of depth. The packing fraction is estimated in sample 1 from the ratio of the electron density at the centres of the Si and Ge regions obtained from the analysis (assuming that at these regions no intermixing has occurred) and the electron density of single-crystal Si and Ge (without defects), respectively. In Fig. 4(*a*) we have plotted the packing fraction of sample 1 as a function of depth obtained at four regions (the Ge, Si, Ge regions of the EDP of the layers and the Si substrate). We approximate the variation of the packing fraction as a linear function of depth (see Fig. 4*a*). For amorphous Si and Ge density up to 30% lower than the bulk crystalline value has been observed depending on the deposition condition. The reduction of electron-density values found in our analysis is within this limit. By taking the ratio of the obtained EDP with the packing fraction we get the EDP which takes into account

the porosity of the film (see Fig. 4*b*). The maximum value of the EDP at ~20 and 100 Å now corresponds to the electron density of the two Ge layers, and the minimum value at ~68 and 200 Å corresponds to the middle layer of Si and the substrate, respectively. In Fig. 4(*b*), for a depth greater than 120 Å, one observes diffusion of Ge into the Si substrate. We observe an interesting feature in the EDP at the Ge–Si interfaces. There is a flat region (having constant electron density) in the EDP at each Ge-on-Si interface (marked by arrows at ~40 and 120 Å) in contrast to a linear variation in the EDP at the Si-on-Ge interface, indicating a sharp interface within the resolution of our measurement.

We have calculated the chemical composition (x) across the depth of the film from the EDP values [for Si_xGe_{1-x} with an electron density of $0.7x + 1.35(1 - x)$ at each point]. This is shown in Fig. 4(*c*). From this figure we observe the formation of at least 16 Å-thick $Si_{0.4}Ge_{0.6}$ alloy at the Ge-on-Si interfaces at $z \simeq 40$ and 120 Å (marked by arrows). This alloy formation is not observed at the Si-on-Ge interface. We feel that in the diffuse interface the alloy $Si_{0.4}Ge_{0.6}$ has formed. $Si_{0.4}Ge_{0.6}$ on Si substrates grown using molecular-beam epitaxy have been studied recently (Ming *et al.*, 1995). The values of x and $1 - x$ which are greater than 1 and negative are due to the linear approximation of the packing fraction. In the case of sample 2, strong intermixing of Si and Ge makes it difficult to extract the packing fraction and as a result the exact composition across the depth, but one can qualitatively obtain the composition from the EDP shown in Fig. 4(*d*).

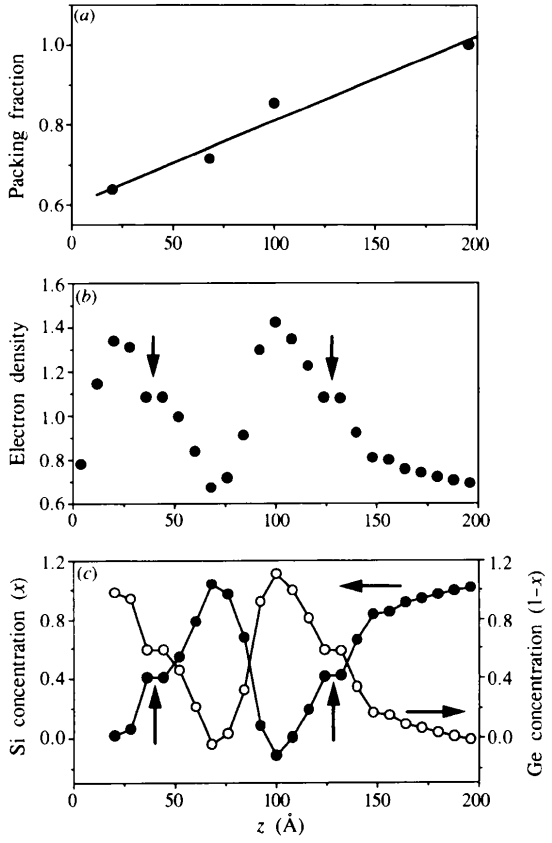

Figure 4
(*a*) Packing fraction as a function of depth for sample 1 (solid line: linear fit). (*b*) Normalized electron density as a function of depth for sample 1. (*c*) Concentration of Si (•) and Ge (○) as a function of depth for sample 1 (see text for details).

5. Conclusions

An X-ray reflectivity study of a thick 16-bilayer III–V semiconductor film and thin Si–Ge trilayers is presented. The layer thicknesses of the $Al_{0.5}Ga_{0.5}As$ and AlAs layers are 465.9 and 471.7 Å, respectively, and apart from the top 80 Å of the film, the electron densities are almost the same as the respective bulk values. We observe an asymmetry of roughness in the AlAs-on-AlGaAs and AlGaAs-on-AlAs interfaces, the r.m.s. roughness of the former being more than the latter. It is interesting to note that although the total bilayer thickness obtained from the X-ray analysis has not differed much from the nominal value (937.6 Å as compared with 940 Å), the thickness of AlGaAs has increased by 25.9 Å and the AlAs thickness has reduced by almost the same amount. This suggests that the extra thickness of the AlGaAs layer is accommodating the interfacial profile, modelled by an error function.

It has been demonstrated that the compositional profile across the depth of a thin film can be obtained by proper analysis of specular reflectivity data. We have used this technique to determine the compositional profile of a Ge–Si–Ge trilayer. We observe that although the interface formed by Si over Ge is sharp, $Si_{0.4}Ge_{0.6}$ alloy is formed at the interface when Ge is deposited over the Si layer.

References

Banerjee, S., Sanyal, M. K., Datta, A., Kanakaraju, S. & Mohan, S. (1996). *Phys. Rev. B*, **54**, 16377–16380.
Bode, M. H. & Ourmazd, A. (1992). *J. Vac. Sci. Technol.* **B10**, 1787–1792.
Chen, Z., Xiao, X., Au, S., Zhou, J. & Loy, M. M. T. (1996). *J. Appl. Phys.* **80**, 2211–2215.
Dandrea, R. G., Duke, C. B. & Zunger, A. (1992). *J. Vac. Sci. Technol.* **B10**, 1744–1753.
Foulon, Y., Priester, C., Allan, G., Garcia, J. C. & Landesman, J. P. (1992). *J. Vac. Sci. Technol.* **B10**, 1754–1756.
Froyen, S. & Zunger, A. (1996). *Phys. Rev. B*, **53**, 4570–4579.
Kohleick, R., Förster, A. & Lüth, H. (1993). *Phys. Rev. B*, **48**, 15138–15143.
Lyakas, M., Arazi, T., Eizenberg, M., Demuth, V., Strunk, H. P., Mosleh, N., Meyer, F. & Schwebel, C. (1995). *J. Appl. Phys.* **78**, 4975–4981.
Ming, Z. H., Huang, S., Soo, Y. L., Kao, Y. H., Carns, T. & Wang, K. L. (1995). *Appl. Phys. Lett.* **67**, 629–631.
Moison, J. M., Guille, C., Houzay, F., Barthe, F. & Van Rompay, M. (1989). *Phys. Rev. B*, **40**, 6149–6162.
Ohkawa, T., Yamaguchi, Y., Sakata, O., Sanyal, M. K., Datta, A., Banerjee, S. & Hashizume, H. (1996). *Physica*, B**221**, 416–419.
Pan, W., Yaguchi, H., Onabe, K., Ito, R., Usami, N. & Shiraki, Y. (1996). *Jpn J. Appl. Phys.* **35**, 1214–1216.
Parratt, L. G. (1954). *Phys. Rev.* **95**, 359–369.
Piecuch, M. & Nevot, L. (1990). *Mater. Sci. Forum*, **59/60**, 93–140.

Presting, H., Kibbel, H., Jaros, M., Turton, R. M., Menczigar, U., Abstreiter, G. & Grimmeiss, H. G. (1992). *Semicond. Sci. Technol.* **7**, 1127–1146.

Rao, T. V. C. & Sanyal, M. K. (1994). *Appl. Surf. Sci.* **74**, 315–321.

Sanyal, M. K., Basu, J. K., Datta, A. & Banerjee, S. (1996). *Europhys. Lett.* **36**, 265–270.

Sanyal, M. K., Datta, A., Srivastava, A. K., Arora, B. M., Banerjee, S., Chakraborty, P., Caccavale, F., Sakata, O. & Hashizume, H. (1997). Submitted.

Sanyal, M. K., Sinha, S. K., Gibaud, A., Huang, K. G., Carvalho, B. L., Rafailovich, M., Sokolov, J., Zhao, X. & Zhao, W. (1993). *Europhys. Lett.* **21**, 691–696.

Schlomka, J. P., Fitzsimmons, M. R., Pynn, R., Stettner, J., Tolan, M., Seeck, O. H. & Press, W. (1996). *Physica*, **B221**, 44–52.

Sinha, S. K., Sanyal, M. K., Satija, S. K., Majkrzak, C. F., Neumann, D. A., Homma, H., Szpala, S., Gibaud, A. & Morkoc, H. (1994). *Physica*, **B198**, 72–77.

Sinha, S. K., Sirota, E. B., Garoff, S. & Stanley, H. B. (1988). *Phys. Rev. B*, **38**, 2297–2310.

Spencer, G. S., Menéndez, J., Pfeiffer, L. N. & West, K. W. (1995). *Phys. Rev. B*, **52**, 8205.

Stall, R. A., Zilko, J., Swaminathan, V. & Schumaker, N. (1985). *J. Vac. Sci. Technol. B*, **3**, 524–527.

Tan, H. H., Jagadish, C., Williams, J. S., Zou, J. & Cockayne, D. J. H. (1996). *J. Appl. Phys.* **80**, 2691–2701.